

## Monitoring solar activity on the far side of the Sun from sky reflected Lyman $\alpha$ radiation

Jean-Loup Bertaux, Eric Quémerais, Rosine Lallement, Elisabeth Lamassoure, Walter Schmidt, Erkki Kyrölä

### ► To cite this version:

Jean-Loup Bertaux, Eric Quémerais, Rosine Lallement, Elisabeth Lamassoure, Walter Schmidt, et al.. Monitoring solar activity on the far side of the Sun from sky reflected Lyman  $\alpha$  radiation. Geophysical Research Letters, American Geophysical Union, 2000, 27 (9), pp.1331-1334. <10.1029/1999GL003722>. <insu-01649835>

HAL Id: insu-01649835

<https://hal-insu.archives-ouvertes.fr/insu-01649835>

Submitted on 27 Nov 2017

**HAL** is a multi-disciplinary open access archive for the deposit and dissemination of scientific research documents, whether they are published or not. The documents may come from teaching and research institutions in France or abroad, or from public or private research centers.

L'archive ouverte pluridisciplinaire **HAL**, est destinée au dépôt et à la diffusion de documents scientifiques de niveau recherche, publiés ou non, émanant des établissements d'enseignement et de recherche français ou étrangers, des laboratoires publics ou privés.

## Monitoring solar activity on the far side of the Sun from sky reflected Lyman $\alpha$ radiation

Jean-Loup Bertaux, Eric Quemerais, Rosine Lallement, and Elisabeth Lamassoure

Service d'Aéronomie du CNRS, BP. 3, 91371 Verrières-le-Buisson, France

Walter Schmidt and Erkki Kyrölä

Finnish Meteorological Institute, P.O. Box 503, FI 00101 - Helsinki, Finland

**Abstract.** Solar active regions are known to be brighter in Lyman  $\alpha$  radiation than the quiet sun. Accordingly, they illuminate more H atoms in interplanetary space through resonance scattering. As we show here, this excess of illumination related to active regions is clearly seen in full-sky Lyman  $\alpha$  maps recorded by the SWAN instrument on board SOHO, including those excesses resulting from active regions which are on the far side of the Sun. Since solar activity is most often connected to solar active regions, this technique could be used in the future to improve the quality of Space Weather forecast, by earlier detection of the birth of a new active region on the far side of the sun, before it comes into Earth's view at the East limb.

### Introduction

Solar activity impacts the Earth's environment through a variety of mechanisms, and it affects occasionally orbiting spacecraft. Efforts are conducted in order to forecast, from solar observations, what could be the impact with a few days advance notice (so-called Space Weather discipline). In addition to CMEs, solar activity is often related to the presence on the surface of the Sun of an active region, which appears rather suddenly and may last for several months. It increases the solar UV and EUV irradiance, which heats the upper atmosphere, both on the 11 year solar cycle and the 27 days (solar rotation) time scales. The resulting atmospheric inflation brings higher densities at a given altitude, increasing the atmospheric drag on orbiting spacecraft and debris. Their orbital parameters are modified, and the short term solar variability effect is a concern in (at least) two areas. High resolution imaging of the ground from space requires an accurate knowledge of the spacecraft position in order to orient the camera in the right direction. The International Space Station, very sensitive to atmospheric drag, must be maneuvered to avoid collisions with other spacecraft and space debris, which orbit must be precisely known to predict potentially dangerous encounters [Lean, 1997].

In the solar UV spectrum (110-400 nm), Lyman  $\alpha$  ( $L\alpha$ ) radiation at 121.6 nm shows the largest variability, at the 100-120 % level [Floyd et al., 1998]. At 121.6 nm the  $L\alpha$  radiation is in

the far UV; it is absorbed by the atmosphere and can be observed only from space. It could be noted however that  $N_2$  is transparent, and  $O_2$  has a narrow window (0.2 nm) of increased transparency (a factor of 100) at  $L\alpha$ . Therefore it penetrates more deeply in the atmosphere (down to 60-70 km). Associated with the fact that it is the most variable solar feature in the solar Far UV, it indicates the importance of this variability for aeronomical processes. In the present article, we discuss the possibility to monitor from space the changes of the solar  $L\alpha$  output from the far side of the sun, which could result in a better forecast system of solar UV/EUV irradiance and atmospheric effect.

The Sun is a strong source of  $L\alpha$  radiation at 121.6 nm, the resonance line of the H atom corresponding to the 1S-2P transition. Therefore, all H atoms in the solar system which are illuminated by the Sun are secondary sources of  $L\alpha$  radiation and can be observed from space. H atoms are found in the upper part of planetary atmospheres, in the extended coma of comets [Bertaux et al., 1973], and in the interplanetary medium [Bertaux and Blamont, 1971; Thomas and Krassa, 1971], all three places where they have been observed in  $L\alpha$  by a number of space instruments since the beginning of space era. The H atoms of interplanetary space are in fact belonging to the interstellar cloud through which the Sun is flowing at the present time [Lallement and Bertin, 1992] at a velocity of 26 km/s, in a direction near the ecliptic plane [Quemerais et al., 1999]. The H density in the solar system is not uniform; ionization by the solar wind and solar EUV creates near the sun a cavity practically void of H atoms. This cavity is elongated in the downwind direction, and its smallest size, found in the upwind direction, is about the size of the Earth's orbit around the Sun (1 Astronomical Unit, A.U.). It extends to 5-10 AU in the opposite, downwind direction (see figure 1).

If the sun's surface were constantly and uniformly bright in  $L\alpha$ , changes in backscattered  $L\alpha$  would occur only when the H atom density distribution is changing where it is observed. This is not the case: the solar  $L\alpha$  output is changing both on 11 year solar cycle and on the 27 days time scale, as documented by a number of space monitoring instruments [Vidal-Madjar et al., 1973; Floyd et al., 1998; Woods and Rottman, 1997]. This latter modulation is obviously related to the solar rotation, and the presence on the surface of brighter regions. It is well known that plages and solar active regions are brighter in the Far UV, and specially in  $L\alpha$  [Fontenla et al., 1998]. Therefore, one single active region on the solar surface will act as a rotating search light, which spot can be seen on the interplanetary H atoms acting as a giant screen (figure 1). In reality,

Copyright 2000 by the American Geophysical Union.

Paper number 1999GL003722.  
0094-8276/00/2000GL003722\$05.00

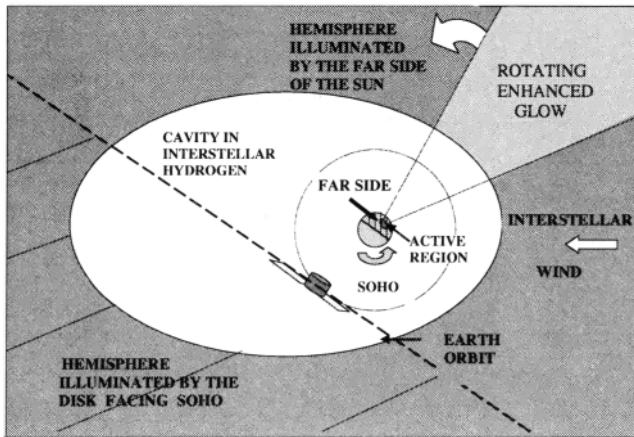


**Figure 1.** Geometry of observations. The sun illuminates in  $L\alpha$  the H atoms (of interstellar origin) in the solar system. An active region on the solar surface which emits more  $L\alpha$  will illuminate more the H atoms which are in view of this active region. This increased illumination (a few percent) of the sky  $L\alpha$  background may be detected by SWAN on board SOHO spacecraft, even if the active region is on the far side of the Sun: the H cloud in the solar system acts as a screen on which the rotating beam from the active region is projected. Ionization by the solar wind creates a cavity void of H atoms which encompasses the SOHO and Earth orbits. A diagonal dashed line separates the two sky hemispheres, illuminated respectively by the far side and the front side of the sun.

the extra beam of light is not strongly collimated as suggested by the sketch of figure 1, but illuminates in  $2\pi$  steradian, most likely with a Lambert's law. In the following, we report 1996 observations of such features from SWAN/SOHO.

### Full Sky Lyman $\alpha$ Observations

The SOHO spacecraft is poised at Lagrange point L1, about  $1.5 \cdot 10^6$  km from Earth on the sun. The primary objective of SWAN instrument [Bertaux et al., 1997] on board SOHO is to determine the latitude distribution of the solar wind from the detailed shape of the sky  $L\alpha$  intensity pattern. For this purpose, the mechanisms of SWAN periscopes are activated 2 or 3 times per week to collect a full-sky map (duration of data collection 24 hr per map). We have analyzed a series of such maps in order to detect the "footprint" of solar active regions on the sky.

On figure 2, the intensity recorded in a fixed celestial direction is plotted as a function of time over 370 days. In principle, there are 3 possible reasons for time variations. The changes of H distribution (due to changes in the solar wind) are slow and are neglected here. The changing location of SOHO in the solar system is the major factor, giving the large sinusoidal trend with a 1 year period. This is because the  $L\alpha$  source glow in the solar system is non-evenly distributed, with a large maximum at 2 A.U. from the sun in the upwind direction. Therefore, the detailed sky pattern depends on the particular position of SOHO along the Earth orbit (parallax effect), and gives an annual pattern of the time variation of the intensity in all directions. The third factor is the non-isotropic solar  $L\alpha$  illumination and 27 days rotation period, which is responsible

for the small wiggles around the mean curve of Figure 2. This mean curve was obtained by a sliding average of the individual points over 50 days (twice the solar rotation in inertial space). Then, the mean curve is subtracted from the data points and the result of subtraction divided by the mean for normalization to 100%. Doing so, the parallax effect is eliminated. Also, the characteristic shape of a map is eliminated, since all the new values obtained for all celestial directions are within 0-10% of unity.

New maps of these normalized intensities can be constructed from each original full sky maps recorded by SWAN, to obtain normalized maps. If the sun were an isotropic source of  $L\alpha$ , these maps would be uniform at value 100. One typical example of a normalized map is shown on figure 3 (obtained from full sky map of July 30, 1996). The sky was divided in two hemispheres separated by the plane containing SOHO, perpendicular to SOHO/sun line. The circle plotted on the right represents the hemisphere opposite to the direction of the sun as seen from SOHO. Therefore, it is illuminated by the side of the sun which is facing SOHO, seen from SOHO. The left circle represents the hemisphere centered on the sun as seen from SOHO, and is therefore illuminated by the far side of the sun. Except for small bright or dark spots which are due to stars, the most conspicuous feature of this map is the presence of a large brighter area centered on the left half of the right hand circle, extending somewhat on the right side of the left circle. We assign this extended brighter area in the sky to the presence of a single active area on the surface of the sun, as shown by the sun EIT image in extreme UV taken on the same day, displayed on the side of figure 3. The active region is slightly south and on the east side of the sun, which comes into view during the solar rotation.

On figure 4 are represented in a similar fashion the SWAN and EIT data for July, 20, 1996, that is to say 10 days before figure 3 data. We note the complete absence of an active region on EIT image, and correspondingly there is no brighter area in the SWAN normalized map on the right, which is illuminated by the sun as viewed from SOHO. However, the SWAN norma-

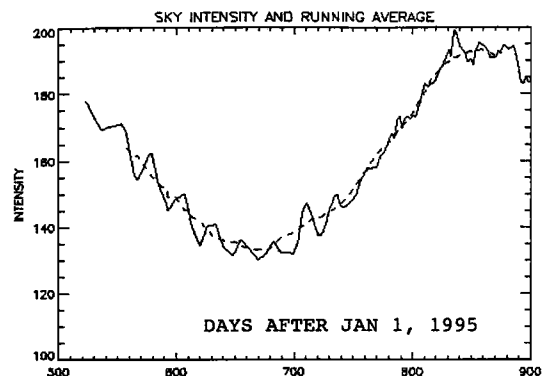


**Figure 2.** Time variation of the  $L\alpha$  intensity recorded by SWAN in a given direction in the sky (ecliptic longitude and latitude:  $320^\circ$  and  $-60^\circ$ ) over 380 days in 1996 and 1997 (solid line). The intensity is in counts/s per  $1^\circ$  pixel. Day 1 is 1st January 1995. The dashed curve is the running average of the data points in a window of 50 days centered on each point. Small wiggles around the running average curve are due to active regions rotating with the sun, emitting more solar  $L\alpha$  and illuminating more the sky in the given direction of sky.

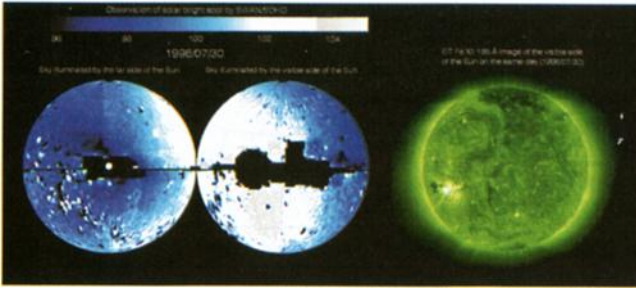


**Figure 3.** This is a comparison of EIT images of the solar disc in EUV wavelength and SWAN normalized images of the sky in  $L\alpha$  taken on July 30, 1996. The full sky images of SWAN are divided in two hemispheres : on the right, it is the anti-solar hemisphere, the one which is illuminated by the sun as viewed from EIT and also seen from Earth. On the left, it is the hemisphere which surrounds the sun (fiducial white circle at center), and therefore a part of the sky which is illuminated by the far side of the Sun. A bright active region is conspicuous on EIT image, and correspondingly there is a brighter wide area in the SWAN image on the right, which is illuminated by the sun as viewed from EIT. The small dark spot at the left of the bright spot in EIT is an artefact. Regions with no SWAN data are black. Small bright or dark spots are artefacts due to stars. The scale of SWAN normalized images is in percent of the running average over 50 days. Longitude coordinates on SWAN maps are reversed w.r.t. the actual sky, for a better understanding of the match to EIT images.

lized map shows a large brighter area on the left circle, representing the hemisphere illuminated by the far side of the sun. Obviously, this brighter area is the result of extra-illumination from the same active region seen with EIT on July 30, but which was 10 days before on the far side of the sun and came into view at the east limb only a few days later (actually, this specific active region was born on July 4, 1996, when it was in view from the Earth).

We have also constructed movies from a succession of normalized maps, on which can be followed easily the rotation of large brighter areas corresponding to solar active regions and the rotation of the sun. Active regions can therefore be easily seen in reflected  $L\alpha$ , even when they are on the far side of the sun.

### Improving Space Weather Forecast with Sky $L\alpha$ mapping .

In the past, latitude distribution of solar  $L\alpha$  illumination has been considered [Cook *et al.*, 1981; Pryor *et al.*, 1992; Pryor *et al.*, 1996], averaging out the 27 days modulation. But here we are interested in the detailed longitude distribution at all times. We have shown that full-sky  $L\alpha$  mapping provides a way to detect the appearance of an active region on the far side of the sun, before it comes in view at the East limb. This method might be used in the future to improve the prediction of the impact of solar activity on the Earth atmosphere and satellite systems (so-called Space Weather). This adds a new tool for Space Weather forecast, in which the solar activity is monitored in order to better predict (short term) what could be the impact on Earth and orbiting spacecraft of an increase of solar activity, in particular the heating of the atmosphere and the in-

creased orbital drag. It is worth noting that it was suggested in the past to use the solar corona itself as a screen for the detection of solar features on the far side of the sun [Beckers and Argo, 1983]. However, the coronal H experiences fast and strong variations, that would complicate the retrieval of the solar surface source. The interplanetary distribution of H is much more stable, and provides therefore a more suitable screen.

The ultimate goal is to determine the distribution of  $L\alpha$  emission as a tracer of active regions on the sun, even on the far side, from full-sky maps. The detailed chain of algorithm remains to be set up. In the present work we used a model-independent method to retrieve the mapping of increased solar illumination, by analyzing directly the data. For an operational system of Space Weather forecast though, the 50 days window centered on the day of the observation could not be used. But a 50 days window ending at the day of the current observation should give also reasonable results for the production of a normalized map, which is an image of the distribution of activity over the whole solar surface. This image is the convolution of the solar surface pattern by the integration over the whole solar disc as seen by each point of the sky.

Alternately, a complete forward modelling of the sky  $L\alpha$  brightness distribution may be used in a loop for data inversion. Starting from a given distribution of  $L\alpha$  emission on the surface of the sun, one computes: 1. the solar  $L\alpha$  flux experienced by all points in the solar system (convolution on the solar disc as seen from each direction), and the primary source function. 2. the final source function (due to radiative transfer of  $L\alpha$  photons in the solar system: this is particularly important for downwind regions). One has to assume a given H distribution in the solar system. 3. the  $L\alpha$  intensity as seen from SOHO. Then the computed map is compared to the observed map, and adjustments are made to the solar surface  $L\alpha$  distribution for a better match.

If this exercise had to be done separately and independently for each daily recorded map, it would be difficult to disentangle the  $L\alpha$  distribution on the solar disc from the distribution of H

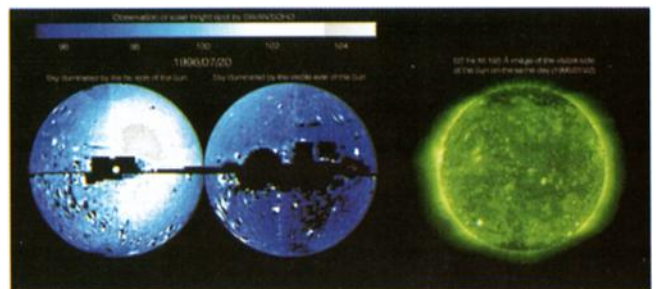


**Figure 4.** Same type of data as for figure 3, obtained ten days before, on July 20, 1996. There is no bright spot on EIT image, and correspondingly there is no brighter area in the SWAN image on the right, which is illuminated by the sun as viewed from EIT. But in the SWAN image on the left side, which corresponds to the sky illuminated by the far side of the sun, there is a wide area which is brighter: it reveals the presence of a bright spot on the far side of the sun. This is the same bright spot that will come into view from EIT a few days later (figure 3).

density in the solar system. In fact, some attempts of forward modelling made in the course of this study failed to reproduce perfectly the sky maps. Systematic departures were found at 5-10 % level, uncorrelated with solar active regions, but rather pointing to small deficiencies of the H model distribution. But analyzing a series of daily maps would be easier. From one map to the next, the  $L\alpha$  intensity change ( in each celestial direction) is the sum of three effects : -the geometrical parallax effect ; -the solar rotation of a fixed pattern distribution of solar surface  $L\alpha$  emission, both effects that are easy to compute with the forward model; and the changes in the non-isotropic solar illumination pattern. The changes of H in the solar system may be neglected because of their longer time scale. New bright areas could be identified, and located rather precisely on the surface of the sun, even on the far side. In this process, the data assimilation techniques that have been developed for meteorological weather forecast could be of great help. Data assimilation is a standard technique used in weather forecast: the meteorological field analyzed for the present time is extrapolated into the future with a numerical model expressing the laws of physics; then, new measurements are mixed with the predictions of the model for an update of the meteorological field (sequential assimilation). In our case, the laws of physics to be considered are mainly the rotation of the sun and the transport of  $L\alpha$  radiation from the surface of the sun to the sky mapper. In conclusion, it could be remarked that this assimilation exercise would also benefit from the direct observation of solar activity on the near side of the sun.

**Acknowledgements.** SOHO (Solar and Heliospheric Observatory) is a mission of international cooperation between ESA and NASA. The construction of the SWAN space instrument was financed by CNES and TEKES. We wish to acknowledge the support of Jean-Yves Prado at CNES for this particular study on Space Weather. We also wish to thank the ESA staff at GSFC for operations, and also Eliane Larduinat, Kim Tolbert and Laura Allen at the Flight Operation Team for their full dedication to the operation of the SOHO instruments. Finally, we wish also to thank Cyril Pennanech and Asko Lehto for data and command management., and Jean-Pierre Delaboudinière for providing the EIT images.

## References

Beckers, J. M. and. Argo, H.V, A Solar Lyman Alpha Coronagraph, SPIE Proceedings, Volume 445, 312, (1983).

- Bertaux, J.L., et al., First Results from SWAN Lyman  $\alpha$  Solar Wind Mapper on SOHO, *Solar Physics*, 175, 737-770 (1997)
- Bertaux, J.L. and Blamont, J.E., Evidence for an extra-terrestrial Lyman  $\alpha$  emission: the Interstellar Wind, J.E. *Astron. Astrophys.*, 11, 200-217 (1971)
- Bertaux, J.L., Blamont, J.E., Festou, M., Interpretation of Hydrogen Lyman  $\alpha$  observations of comets Bennett and Encke, *Astron. Astrophys.*, 25, 415-430 (1973).
- Cook, J.W., Meier, R.R, Brueckner, G.E., and VanHoosier, M.E., Latitudinal Anisotropy of the Solar Far Ultraviolet Flux: Effect on the  $L\alpha$  Background *Astron. Astrophys.*, 97, 394 (1981)
- Floyd, L.E., et al., Solar Cycle 22 UV spectral irradiance variability: current measurements by SUSIM UARS, *Solar Physics* 177, 79-87 (1998)
- Fontenla, J., Reichmann, E.J., and Tandberg-Hanssen, E., The Lyman-Alpha line in various solar features. I. Observations, *Astrophys. Journal*, 329,464 (1988).
- Lallement, R. and Bertin, P., Northern Hemisphere observations of the LISM: Possible detection of the Local Interstellar Cloud, *Astron. Astrophys.*, 266, 479 (1992)
- Lean J. The Sun's variable radiation and its relevance for Earth, *Annu. Rev. Astron. Astrophys.* 35, p.33 (1997)
- Pryor, W.R., et al., The Galileo and Pioneer Venus ultraviolet spectrometer experiments : solar Lyman  $\alpha$  latitude variation at solar maximum from interplanetary Lyman- $\alpha$  observations, *Astrophys. J.*, 394, 363, (1992)
- Pryor, W.R., et al., Latitude variations in interplanetary Lyman- $\alpha$  data from the Galileo EUVS modeled with solar He 1083 nm images. *Geophys.Res.Letters* 23 (15), 1893, (1996)
- Quemerais, E., et al, Interplanetary Lyman  $\alpha$  Line profiles derived from SWAN/SOHO H Cell measurements I. The Full Sky Velocity Field, *J. Geophys. Res.*,104, 12585-12603 (1999).
- Thomas, G.E. and Krassa, T., Ogo-5 measurements of the Lyman  $\alpha$  sky background, *Astron. Astrophys.*, 11, 218 (1971)
- Vidal-Madjar, A., Blamont, J.E. and Phissamay, B., Solar Lyman  $\alpha$  changes and related hydrogen density distribution of the Earth's exobase (1969-1970), *J. Geophys. Res.*, 77,115 (1973)
- Woods, T.N. and Rottman, G.J, Solar Lyman  $\alpha$  irradiance measurements during two solar cycles, *J. Geophys. Res.* 102, p.8769, (1997)

J.L. Bertaux, E. Quemerais, R.Lallement (e-mail: bertaux@aerov.jussieu.fr, quemerais@ aerov.jussieu.fr, lallement@aerov.jussieu.fr)  
 W.Schmidt, E. Kyrölä (e-mail: walter.schmidt@fmi.fi, erkki.kyrola@fmi.fi)

(Received December 2,1999; Accepted January 27, 2000)